

Coupled Atmosphere–Wildland Fire Modelling

Jean Baptiste Filippi¹, Frédéric Bosseur¹, Céline Mari², Christine Lac³,
Patrick Le Moigne³, Bénédicte Cuenot⁴, Denis Veynante⁵, Daniel Cariolle⁴ and
Jacques-Henri Balbi¹

¹ SPE – CNRS UMR 6134, Campus Grossetti, BP52, 20250 Corte, France

² LA – CNRS UMR 5560, OMP, 14 Avenue Edouard Belin, 31400 Toulouse, France

³ CNRM, 42, Avenue Gaspard Coriolis, 31057 Toulouse Cedex 01, France

⁴ CERFACS, 42, Avenue Gaspard Coriolis, 31057 Toulouse Cedex 01, France

⁵ EM2C – CNRS UPR 288, ECP, Grande Voie des Vignes, 92295 Chatenay-Malabry, France

Manuscript submitted 31 December 2008; in final form 4 June 2009

Simulating the interaction between fire and atmosphere is critical to the estimation of the rate of spread of the fire. Wildfire's convection (i.e., entire plume) can modify the local meteorology throughout the atmospheric boundary layer and consequently affect the fire propagation speed and behaviour. In this study, we use for the first time the Méso-NH meso-scale numerical model coupled to the point functional ForeFire simplified physical front-tracking wildfire model to investigate the differences introduced by the atmospheric feedback in propagation speed and behaviour. Both numerical models have been developed as research tools for operational models and are currently used to forecast localized extreme events. These models have been selected because they can be run coupled and support decisions in wildfire management in France and Europe. The main originalities of this combination reside in the fact that Méso-NH is run in a Large Eddy Simulation (LES) configuration and that the rate of spread model used in ForeFire provides a physical formulation to take into account the effect of wind and slope. Simulations of typical experimental configurations show that the numerical atmospheric model is able to reproduce plausible convective effects of the heat produced by the fire. Numerical results are comparable to estimated values for fire-induced winds and present behaviour similar to other existing numerical approaches.

DOI:10.3894/JAMES.2009.1.11

1. Introduction

Wildland fire initiation and spread are known to be heavily influenced by wind (Clements et al., 2006; Santoni et al., 2006). The direction of the spread, propagation speed and fire plume are the result of strong interactions between the wildfire and the atmosphere occurring at different scales (turbulent mixing of air and gas in the front, large eddies formed near the front, fire-induced winds at the scale of a valley up to the creation of pyro cumulus).

The numerical coupling of a fire model with an atmospheric model has already been the subject of numerous studies, starting from the work (with static fire) of Heilman and Fast (1992) to the more recent work of Clark et al. (2004), that proposes a simplified model of fire spread tailored for a Canadian forest (Rothermel, 1972), coupled with an extension of the atmospheric fluid dynamic model of Clark (1977, 1979), Clark and Hall (1996) and more recently with the Weather Research & Forecasting Model (WRF) meso-scale mode (Skamarock and Klemp, 2007). While these efforts are effective at simulating the coupled

effects at the scale of a large fire (several square kilometres) with a high degree of fire front precision, the use of the Rothermel model should be subject to caution as the effects of wind and slope to the rate of spread (RoS) are expressed as coefficients that are experimentally fitted to wind values *as if the fire was not there*.

Other studies are more focused on combustion processes with a detailed physical formulation of the fire front. With the Wildland version of the Fire Dynamics Simulator (FDS), Mell et al. (2007) obtained a good numerical correspondence with a real prescribed burning experiment of Australian grassland (Cheney and Gould, 1995). With HIGRAD/FIRETEC, Linn et al. (2002) were able to perform several numerical investigations with different topography and wind conditions. While these efforts are necessary to understand the mechanisms driving the fire spread, the analysis of large

To whom correspondence should be addressed.

Jean Baptiste Filippi, SPE – CNRS UMR 6134, Campus Grossetti, BP52, 20250 Corte, France
batti.filippi@gmail.com

fires would require large computing facilities because of the scales on which the simulation must be run.

This study presents the first coupled simulation using two numerical models, Méso-NH and ForeFire, developed to serve research purposes for operational models. In an approach similar to Clark et al. (2004), this meso-scale atmospheric model and the reduced physical front-tracking wildfire model are coupled to investigate the differences introduced by the atmospheric feedback in terms of propagation speed and behaviour.

The main originalities of this combination reside in the fact that Méso-NH is run in a Large Eddy Simulation (LES) configuration and that the RoS model used in ForeFire provides a physical formulation to take into account the effect of wind and slope.

Both models can already be used at the scale of a large fire, and the long-term objective of the coupled model is to be able to take into account the complex topography, fuel and fuel break distribution typical of the Mediterranean region.

The first section of the article presents short descriptions of the atmospheric model, fire propagation model and coupling method. Simulation results shown in the second section are consistent with estimated fire-induced wind speed compiled by Trelles and Pagni (1997) and simulated front behaviour is coherent with previous simulations from Linn et al. (2007) and Clark et al. (1996).

2. Numerical models and coupling method

The coupled model is composed of a meso-scale atmospheric model and a fire RoS model that is used to advect fire contours using a front-tracking method.

a. Atmospheric model

The anelastic non-hydrostatic meso-scale model Méso-NH (Lafore et al., 1998) is used to integrate the coupled fire-atmospheric winds that advect the fire front over the surface. The model is intended to be applicable to all scales ranging from large (synoptic) scales to small (large eddy) scales and can be coupled with an on-line atmospheric chemistry module. In the present study, Méso-NH is run in the LES configuration ($\Delta x = 30\text{m}$) mode without chemistry. The turbulence parameterization is based on a 1.5-order closure (Cuxart et al., 2000), with a prognostic equation for turbulent kinetic energy in 3D (which allows for the resolution of the horizontal turbulent fluxes). Open boundary conditions were chosen. Momentum variables are advected with a centred fourth-order scheme, while scalar and other meteorological variables are advected with a so-called monotonic Piecewise Parabolic Method (Woodward and Colella, 1984). The model is coupled with an externalized surface model which includes vegetation (Noilhan and Planton, 1989) and urban dynamics (Masson, 2000). Fire feedback is introduced in the simulation by the externalized surface, with a fire RoS model used to advect the fire front contour.

b. Fire spread model

The physical fire spread model forecasts the RoS using a formulation described in Balbi et al. (2007). It has been developed to provide an analytical formulation of the propagation speed given slope, wind speed and fuel parameters.

The main hypothesis of the model is that the fire front is acting as a tilted radiant panel that is heating the vegetation in front of it, vaporizing the water content before entering into pyrolysis. This hypothesis is used in most operational fire spread models, such as the widely used Rothermel model (Rothermel, 1972).

In the Rothermel model, slope and wind effects are taken into account as additive empirical fuel-dependent coefficients, fitted for mid-flame winds speed *as if the fire was not here*. In the proposed RoS model, wind and slope effects are explicitly taken into account by calculating a flame tilt angle with a vector method and therefore may be more appropriate for use in a coupled configuration (Sharples, 2008).

In order to provide a simplified formulation of the RoS under different conditions, it is also assumed that the radiant factor (denoted A , ratio of radiant to total heat release) decreases with the surface/volume ratio of the flame and that the gas flow speed and direction in the flame are given by the vectorial sum of the wind speed with a given vertical gas velocity due to buoyancy and combustion. With these hypotheses there is a minimal set of parameters that need to be identified for each fuel type in order to characterize how the fuel is reacting to radiation and the quality of combustion.

Calculation of the flame tilt angle, γ , is presented in Fig. 1.

Formulation of γ is given by:

$$\tan \gamma = \tan \alpha + \frac{U}{u_0}, \quad (1)$$

with α , the local slope angle in degrees and U the wind velocity normal to the propagation (in ms^{-1}). R , the RoS (in ms^{-1}), is obtained by adding the nominal speed of the fire

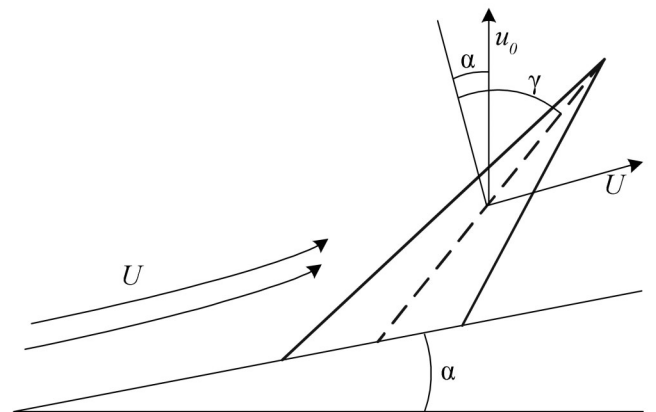


Figure 1. Calculation of the flame tilt angle.

to the speed due to the tilted flame radiating in the vegetation in the direction of the propagation. R is given by:

$$R = R_0 + A \frac{R(1 + \sin \gamma - \cos \gamma)}{1 + \frac{R}{r_0} \cos \gamma}. \quad (2)$$

Parameter A is the radiant factor (A is high if much of the energy generated by combustion is radiated by the front). Parameter r_0 is a speed factor due to radiation (in ms^{-1}) that is dependent on the flame thickness. Parameter R_0 , the RoS without wind and slope (in ms^{-1}), is mainly dependent on the actual quantity of water inside the vegetation. Finally u_0 , the vertical gas velocity in the flame without wind and slope (in ms^{-1}), is used to represent the heat release rate inside the flame.

The model output is the RoS available for every direction. Normal wind and slope values are calculated given the actual direction of portions of the front. The RoS for every portion of the front is then used by a front-tracking method for the simulation of the fire perimeter.

c. Front tracking

The front-tracking method used to simulate the advance of the front derives from a method of markers (Lallemand et al., 2007; Du et al., 2006). This Lagrangian method, presented in Fig. 2, works by moving a set of points or markers located at the interface line, each of the markers being connected to the next marker by a piecewise linear segment; at each step markers are moved according to the speed function R in the direction of the normal to the front at this point. Markers are redistributed along the front if separated by more than a quantum distance Δq . This method has been selected because of its computational efficiency, and the ability to simulate the propagation of an interface at the high

resolution (a few metres) needed to take into account different vegetations, roads, houses and fire breaks over a large area typical of a wildfire accident (hundreds of square kilometres).

Reconstruction of the front fire width is performed by projecting the future location of the marker along the propagation vector after the burning duration of the fire or “Residence Time”, denoted R_T .

The local wind is interpolated using a bi-cubic method at the very location of the markers distributed along the back fire line. It is considered that the wind at this location represents the actual wind that is tilting the flame.

The local slope angle is interpolated from the elevation difference between the marker location and the projected location of the marker.

d. Coupling method

Wind matrices are updated at each atmospheric time step and the wind is assumed to be constant during the entire duration of the step. In order to provide a feedback from the fire to the atmosphere, three different surface matrices are generated from the wildfire model to force the atmospheric model at the first (ground) level: sensible heat fluxes in Wm^{-2} , flux of water vapour in kg m^{-2} and radiant temperature in K.

Results for each grid cell are extracted by polygon clipping the surface of the intersection between the burning area of the front shape (denoted S_b) and the total cell area, denoted S_c ($\Delta x \Delta y$) (Fig. 3). The burning ratio for each atmospheric grid cell, denoted R_b , is given by:

$$R_b = \frac{S_b}{S_c}, \quad (3)$$

so that the burning portion of the cell ranges from 0 (no fire) to 1 (all burning).

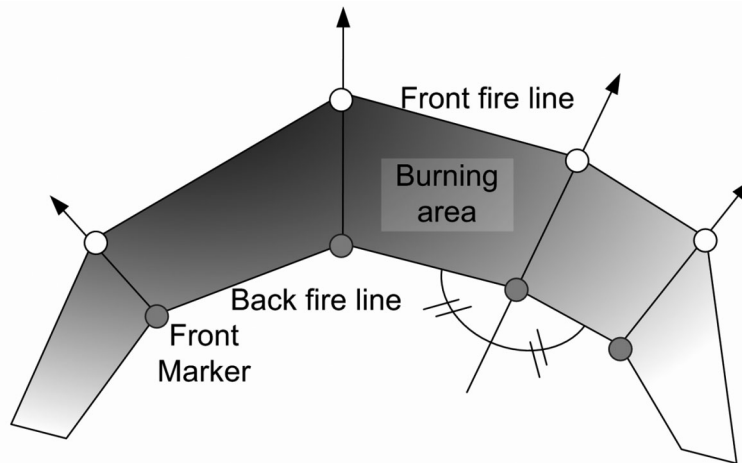


Figure 2. Front-tracking method of markers. Grey circles represent markers along the back fire line. Arrows show the propagation vector (bisector of the local angle at the marker). White circles along the front fire line show the projected locations of the markers after the local burning duration.

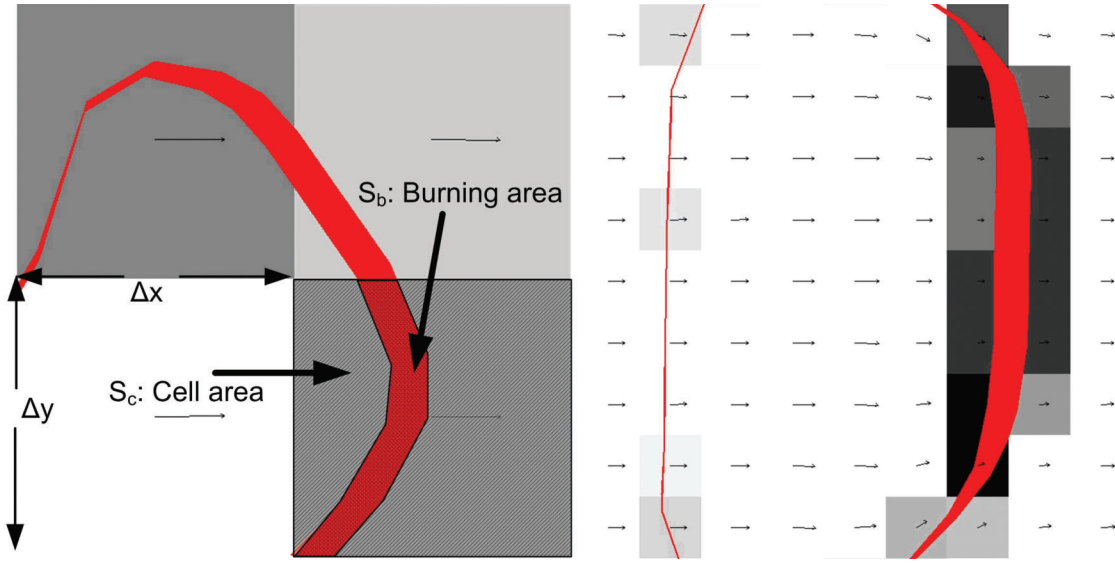


Figure 3. Integration of burning area. The red shape represents the fire front. Integration is performed on each atmospheric cell (shades of grey correspond to the burning (S_b) to total cell area ($S_c = \Delta x \Delta y$) ratio, black is S_b max).

Feedback to the atmosphere is performed by calculating an equivalent radiant temperature, convective heat fluxes and water vapour fluxes matrices from the burning matrix.

As only a portion of the cell is burning, an equivalent radiant temperature (T_e) for the whole cell is averaged from a nominal flame temperature (T_n) and the soil temperature from the atmospheric model (T_s). T_e is deduced from the Stefan–Boltzman equation as:

$$T_e = \sqrt[4]{(1 - R_b)T_s^4 + R_b T_n^4}, \quad (4)$$

so that the total amount of radiant energy for the cell is equivalent to the energy radiated from the soil area added to the energy of the flame area. One of the main assumptions made here is that the flame front can be represented as a rectangular box emitting radiation as a blackbody surface; this common simplification is discussed in detail in Sullivan et al. (2003). The nominal flame temperature (T_n) used for the study (1000K) is taken from the lowest values reported in an experiment by Sullivan et al. (2003) and performed using a propane-based bushfire simulator. Radiant temperature is chosen from the lowest values because the blackbody assumption is known to overestimate radiant heat (Knight and Sullivan, 2004). Investigation on a more precise radiant-coupling scheme is the subject of ongoing work, but the proposed straightforward approach has the advantage of a low computational cost.

Equivalent convective heat fluxes (Q_e) in Wm^{-2} , corresponding to the energy of the hot gaseous column over an atmospheric cell, is approximated from a nominal convective heat flux (Q_n) with:

$$Q_e = R_b Q_n. \quad (5)$$

Finally, equivalent water vapour fluxes (Wv_e) in kg m^{-2} , representing the amount of water vapour evaporated from the vegetal stratum, is interpolated over an atmospheric cell from nominal water vapour content (Wv_n) with:

$$Wv_e = R_b Wv_n. \quad (6)$$

Those matrices are passed to the atmospheric model at every atmospheric time step, just before updating the wind matrix used to advect the fronts.

3. Experimental set-up and simulation results

Insufficient data and difficulties conducting full-scale experiments limit verification of coupled atmosphere–wild-land fire modelling. As such, fire-induced winds cannot be directly measured; instead the maximum wind velocity near the front can be compared with the actual ambient wind over the area.

Large-scale experiments were carried out in the sixties to investigate the effects of mass fires, most notably project FLAMBEAU in the USA (Countryman, 1969; Palmer, 1969), operation EUROKA in Australia, (Adams et al., 1973) and more recently the Canada Mass Fire Experiment (Quintiere, 1989).

In a study from 1997, Trelles and Pagni (1997) analysed fire-induced winds from burning wooden houses in a real wildfire accident (1991 Oakland Hills fire). Classical plume theory and the McCaffrey model (McCaffrey, 1986) were used to investigate the effect of large (259) sources of 50 Mw fires ignited almost simultaneously in an area of roughly 50 Ha. In the same study, Trelles and Pagni also compiled different wind velocities estimated from the literature. Data from this study show that maximum horizontal velocities

Table 1. Experimental configurations for the simulations.

Name	Number of Ignitions	Ignition type	Wind	Slope
CONF1	1	Point	3m.s ⁻¹	10%
CONF2	2	Point	3m.s ⁻¹	0%
CONF3	1	400m line	3m.s ⁻¹	10%

ranged between 4–12 ms⁻¹ for the smaller fires (semi-controlled Canada Mass Fire Experiment) and 16–22 ms⁻¹ for the larger fires (50000 piles of fuel ignited simultaneously in project FLAMBEAU). Moreover, in the real wildfire studied by Trelles and Pagni, the vertical wind velocities ranged from 14 ms⁻¹, for the early stages of the Oakland Hills fire, to 26 ms⁻¹, when fire reached maximum intensity and all heat sources had been activated.

Although they provide hints as to the range of velocities expected in the plume for fires of comparable intensities, none of these studies provides direct measurements of fire-induced winds, and are biased by the use of the semi-empirical McCaffrey model.

In terms of fire behaviour, several simulations of idealized configurations have been performed by Linn et al. (2007), Coen et al. (2001) and Clark et al. (1996) to numerically investigate typical atmospheric feedback on the fire line. It appears from these simulations that the magnitude of the feedback is dependent not only on the fire intensity (Linn et al., 2007), but also on the ambient wind speed, with a stronger relative feedback when the ambient wind is weak (Clark et al., 1996). In those simulations, the most significant coupled effect of the fire on the atmosphere is the initiation of strong convection, which creates an area of wind convergence under the fire plume. In both studies, forecasting the location and strength of the fire plume was of prime importance to the estimation of the effective feedback between the fire and the atmosphere.

In order to simulate qualitatively comparable fires in terms of intensity and configuration, three model configurations have been selected: a case with a slope in the direction of the wind and a point ignition (CONF1), representing a small fire, a case with no slope but two ignition points separated by 100 metres (CONF2), to investigate fire feedback between fires and fire plume convergence, and a case with a slope and a line ignition about 400 metres long (CONF3), representing a strong fire. Configurations for the three fires are available in Table 2. All simulations have been run with and without coupling (with a constant wind field and no fluxes or radiation forcing). The resolution is such that the fire width is

comparable to the atmospheric grid size, here $\Delta x = \Delta y = 30$ metres, so that the fire heat release is not diluted over a large area. In all simulations, the domain was 1.2 km by 1.2 km in size and 1.2 km high. The atmospheric time step for the simulation was set to 0.5 seconds with a Δq for the front of 2 m.

Table 2 presents the model parameters for all simulations, based on mean values deduced from experimental studies (Santoni et al., 2006). In this experiment, the vegetation consisted of shrubs, with an average dry fuel load of 7 kg m⁻².

For all experiments, the atmospheric model background wind field was 3 ms⁻¹ and of constant height; this relatively weak value is typical of prescribed burning. Diagnostics for the plume were performed by injecting, at ground level, a passive scalar tracer with a concentration and a distribution equal to the burning ratio of each grid point and for each atmospheric time step.

Figure 4.a presents the simulation of a point ignition with a slope after 600 seconds of simulation (CONF1). Significant differences between the front from the coupled and the front from the non-coupled simulations are observed in terms of fire shape and RoS. The strong heat flux generates a localized wind velocity of 5.4 ms⁻¹ in the direction of the slope that increases the head fire RoS from 0.3 ms⁻¹ (without coupling) to 0.5 ms⁻¹ (with coupling). In this configuration, it appears that the fire is creating an area of confluence near the fire head, just under the hot air column, an effect similar to the effect simulated by Linn et al. (2007) and Coen et al. (2001). The creation of this hot air column had the effect of collecting winds on the fire sides, thus creating an acceleration of the winds near the front, increasing the RoS.

The vertical section (Fig. 4.b) presents a well-defined plume with a maximum wind velocity of 7.1 ms⁻¹ in the plume and a maximum concentration of tracer very near the front, showing how quickly the fire would have been dissipated by fire plume convection. A significant concentration of tracer is found at a height of 240 metres, where the atmosphere remains unaffected by the fire forcing. With respect to fire burning experiments, the simulated values are comparable to those estimated for the smaller fires (50 Kw m⁻² in the early stages of the Oakland Hills analysis using the McCaffrey model).

Figure 5.a presents the simulation of the two-point ignition case without slope (CONF2) after 600 seconds of simulation. Compared with the previous experiment, the local wind velocity is increased to 5.5 ms⁻¹ in the direction of the wind, increasing the head fire RoS from 0.3 (without

Table 2. Experimental parameters, with A : Radiant factor, R_0 : rate of spread without wind and slope, r_0 flame thickness speed factor, u_0 : flame gas velocity, R_T : fire residence time, Q_n : nominal heat flux, Wv_n : nominal water vapour flux and T_n : nominal radiant temperature.

A	R_0	r_0	u_0	R_T	Q_n	Wv_n	T_n
1.5	0.1m.s ⁻¹	0.01m.s ⁻¹	5m.s ⁻¹	30s	150kW.m ⁻²	0.1kg.m ⁻²	1000K

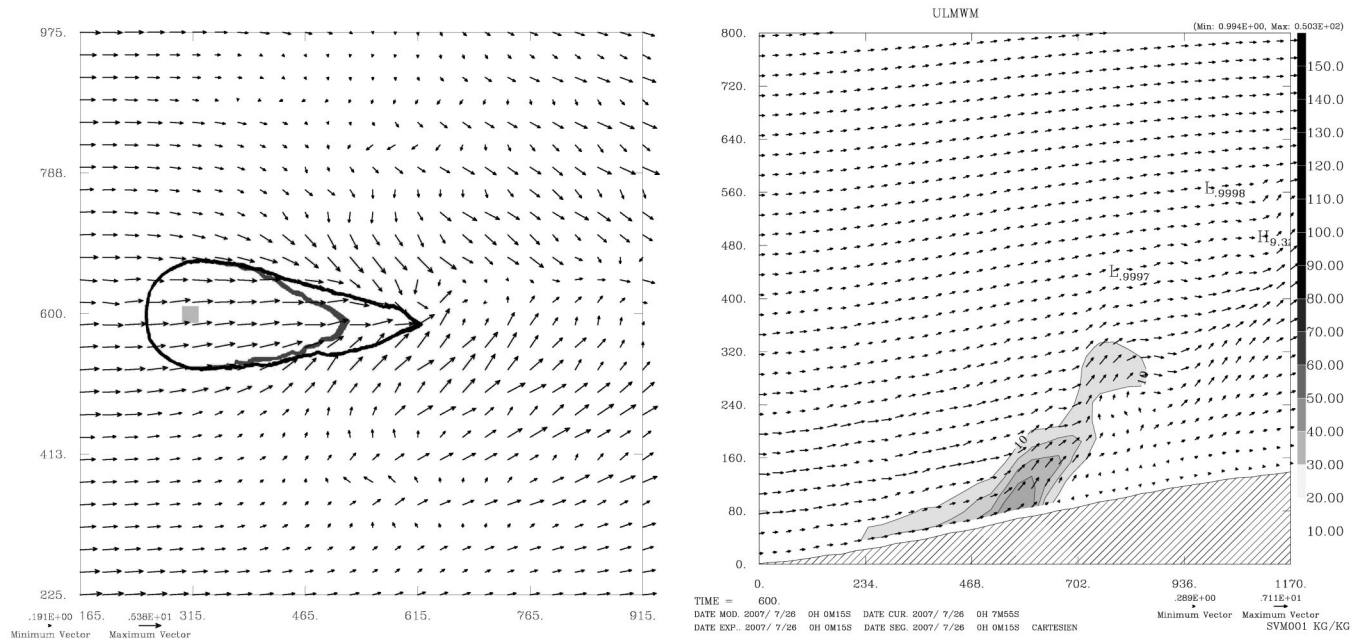


Figure 4. CONF1 (a) Horizontal section (x/y) at Z=10m, fire line propagation after 600 seconds for the coupled (black) and non-coupled (grey) simulations. Arrows denote the wind vectors of the coupled case. A light-grey square represents the initial ignition point for both cases. (b) Cross-section (x/z) of the coupled case at Y=600m, shading represents concentration of the injected passive tracer.

coupling) to 0.6 ms^{-1} (with coupling). In this case, the same wind confluence (plume base) area can be found over of the front. Compared with the non-coupled case, the coupled case reacts rapidly to the junction of the two fires by generating a zone of high wind velocity, creating a peak in

the front instead of two merged ellipsoids. It appears that one larger fire plume has been initiated instead of two distinct plumes, with side winds created by the hot air column having the effect of merging the two fire heads. Early work from Clark et al. (1996) also found that the RoS

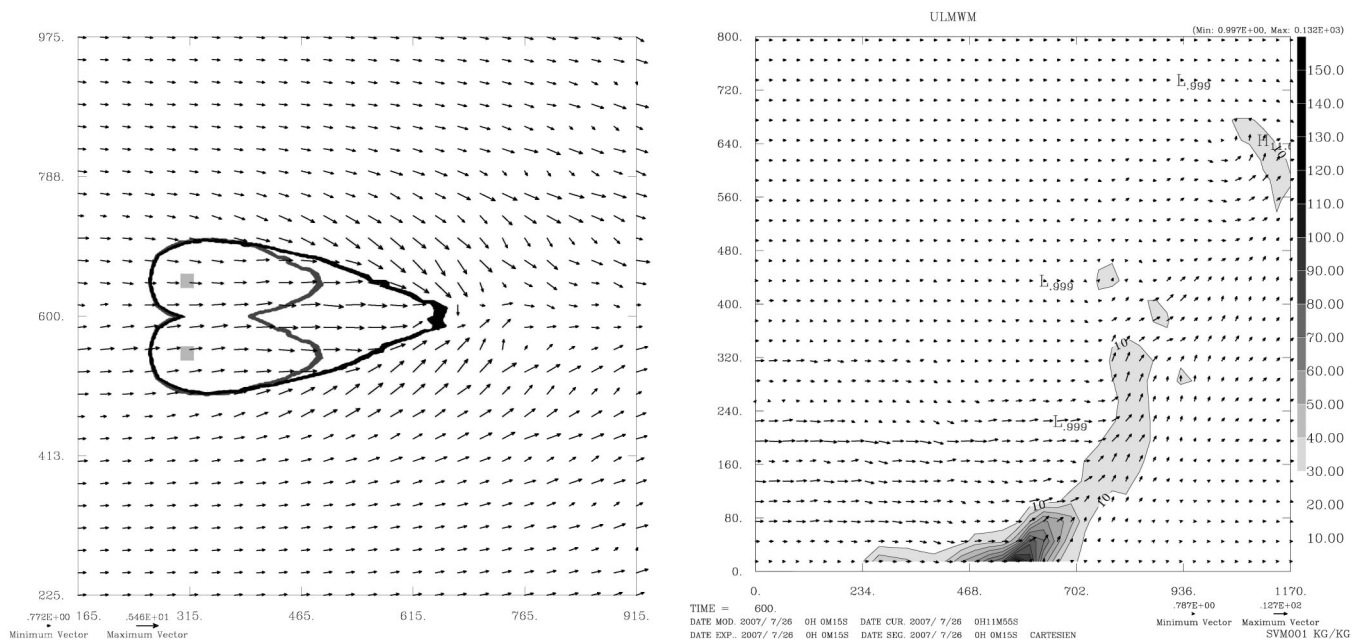


Figure 5. CONF2 (a) Horizontal section (x/y) at Z=10m, fire line propagation after 600 seconds for the coupled (black) and non-coupled (grey) simulations. Arrows denote the wind vectors of the coupled case. A light-grey square represents the initial ignition points for both cases. (b) Cross-section (x/z) of the coupled case at Y=600m, shading represents concentration of the injected passive tracer.

is much larger in a double fire experiment when a forward fire plume can entrain a rear one and becomes a single plume.

The same effect of wind acceleration towards the plume base can be observed here, with a stronger effect on the RoS due to the two fronts merging.

The vertical section (Fig. 5.b) presents a well-defined plume with a maximum wind velocity of 12 ms^{-1} and an area of maximum tracer concentration found at a height of 320 metres.

Finally Fig. 6.a presents the simulation in the case of a 400-metre-long line ignition with slope (CONF3) after only 200 seconds of simulation.

Compared with the previous experiments, the local wind velocity reaches 7.7 ms^{-1} near the fire front, increasing the head fire RoS from 0.25 (without coupling) to 1 ms^{-1} (with coupling).

Owing to the much greater amount of energy released by fire in the CONF3 simulation, the results seen in Fig. 6 are more representative of the RoS and plume of a large wildfire. The vertical section (Fig. 6.b) presents a well-defined plume with a maximum wind velocity of 19 ms^{-1} in the plume, consistent with the early stage of the large wildfire studied by Trelles and Pagni (1997), when just a few of the heating sources were ignited. The maximum tracer concentration reaches an altitude of 830 metres, suggesting that the smoke is advected directly into higher atmosphere by strong fire-induced convection.

In this configuration, the area of confluence of the winds under the plume is located 100 m ahead of the fire front,

generating strong side winds towards the centre of the front that reduce the width of the front from 400 m (ignition line length) to 150 m. Similar behaviour, with a fire front evolving towards a peak instead of a large line, was obtained by Linn (2007) on a uphill forest fire simulation using FIRETEC. In this case, stronger convection in the plume generated a strong uphill wind that moved the plume base in the slope direction. The greater acceleration of the coupled case (compared with weaker fires produced in the non-coupled simulations) may be explained by the displacement of the fire plume and the fire front being directly exposed to the fire-induced winds.

For the three simulations, predicting the location and strength of the fire plume prove to be critical to forecasting the front spread and behaviour. The coupled model was able to simulate fire convection and the acceleration of the fire front due to the acceleration of winds collected by the plume. In terms of vertical wind within the plume, the range of values simulated by the proposed model ($7\text{--}19 \text{ ms}^{-1}$) is consistent with previous analyses of medium to large wildfires ($14\text{--}26 \text{ ms}^{-1}$). In terms of behaviour, the model was able to reproduce fire convergence (CONF2) and the dependence of RoS upon the fire intensity, with the greatest RoS achieved in CONF3.

All simulations were performed on a bi dual-core Intel Xeon processor running at 3 Ghz with 8Gb of memory. The calculation time for each run was about 4 hours for 3000 seconds of simulation. The calculation of the fire front displacement only accounts for 5 seconds of computer time, while the coupling requires 100 seconds, mainly to perform

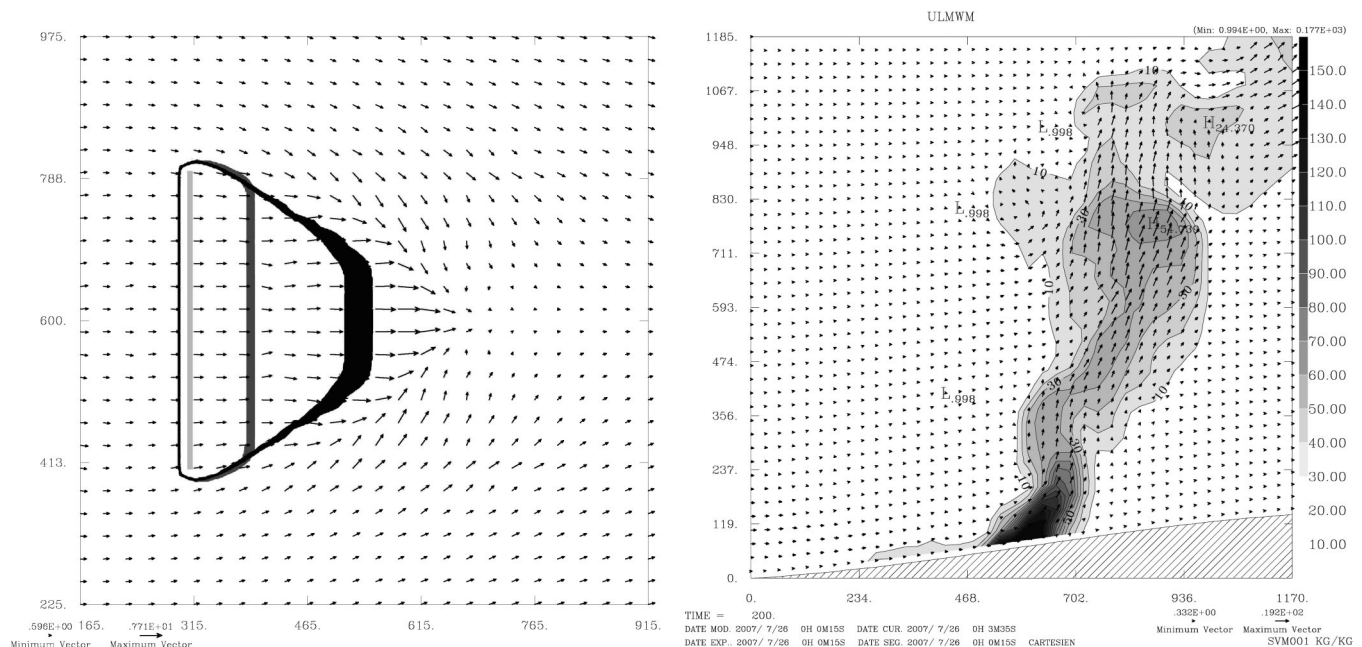


Figure 6. CONF3 (a) Horizontal section (x/y) at Z=10m, fire line propagation after 200 seconds for the coupled (black) and non-coupled (grey) simulations. Arrows denote the wind vectors of the coupled case. Light-grey line represents the initial ignition for both cases. (b) Cross-section (x/z) of the coupled case at Y=600m, shading represents concentration of the injected passive tracer.

input/output operations for the duration of the run. While still fast on a relatively modest computer, the scale of the simulation (about a square kilometre, for about an hour) is still far from the scale of a large wildfire (hundreds of square kilometres, for about a day). However, our primary objective here was to explore the feasibility of coupled atmosphere-wildland fire simulations with Méso-NH and ForeFire. Realistic large-scale simulations are the subject of ongoing work and require a computer between 100 and 1000 times faster than the test platform, a computational power currently only available on supercomputers in National Centres.

4. Conclusions

This paper presented the MésoNH-ForeFire model of wildland fire spread. By using a simple coupling method, the atmospheric model is able to simulate the atmosphere dynamic induced by the fire and the subsequent effects on the RoS with meaningful results. Three simulations of idealized cases were performed, with fire-induced convection appearing to strongly influence fire spread.

In the most intensive fire simulation (large fire line ignition), winds are accelerating about an order of magnitude faster than the ambient wind near the front. Simulated values for the fire-induced wind are consistent with the analysis of large fires using standard plume theory (more than 50-m-long fire line with intensity exceeding 50 Kw m^{-2}). Simulated propagations in the coupled cases also show patterns (creation of a peak in the front and convergence of fire heads) similar to existing numerical fire/atmosphere experiments from the literature.

Injection of passive tracers into the fire at the ground level shows a fire plume rising to an altitude of 830 metres with the most intense fire. Unlike the smaller model fire, the larger line ignition model generated enough convection to reach this altitude. This result suggests a critical fire size for emission of smoke high in the atmosphere that could be further explored by using several fire intensities, several idealized wind profiles (with strong and weak winds) and several atmospheric boundary layer types (thick, thin, stable and turbulent) to determine which conditions will result in long-distance transport of smoke.

Further enhancements are also planned to perform simulation with the online chemistry module of Méso-NH in order to investigate fire smoke and particle transport.

Acknowledgements: This research was supported by PEPS-07_36 from the French National Centre of Scientific Research (CNRS). The authors would like to thank the anonymous reviewers whose suggestions and corrections helped to improve the paper.

References

- Adams, J. S., D. W. Williams, and J. Tregellas-Williams, 1973: Air Velocity, Temperature, and Radiant-Heat Measurements within and around a Large Free-burning Fire. *14th Int'l Symposium on Combustion*, p. 1046–1049. The Combustion Institute, P.A.
- Balbi, J. H., J. L. Rossi, T. Marcelli, and P. A. Santoni, 2007: A 3D physical real-time model of surface fires across fuel beds. *Combustion Science and Technology*, **179**, 2511–2537, doi:10.1080/00102200701484449.
- Cheney, N. P., and J. S. Gould, 1995: Fire growth in grassland fuels. *J. Wildland Fire*, **5**, 237–347, doi:10.1071/WF9950237.
- Clark, T. L., 1977: A small-scale numerical model using a terrain following coordinate transformation. *J. Comput. Phys.*, **24**, 186–215, doi: 10.1016/0021-9991(77)90057-2.
- Clark, T. L., 1979: Numerical simulations with a three-dimensional cloud model: lateral boundary condition experiments and multi-cellular severe storm simulations. *J. Atmos. Sci.*, **36**, 2191–2215, doi: 10.1175/1520-0469(1979)036<2191:NSWATD>2.0.CO;2.
- Clark, T. L. and W. D. Hall, 1996: On the design of smooth, conservative vertical grids for interactive grid nesting with stretching. *J. Appl. Meteor.*, **35**, 1040–1046, doi: 10.1175/1520-0450(1996)035<1040:TDOSCV>2.0.CO;2.
- Clark, T. L., M. A. Jenkins, J. Coen, and D. Packham, 1996: A Coupled Atmospheric-Fire Model: Convective Froude number and Dynamic Fingering. *International Journal of Wildland Fire*, **6**, 177–190, doi:10.1071/WF9960177.
- Clark, T. L., J. Coen, and D. Latham, 2004: Description of a coupled atmosphere-fire model, *International J. of Wildland Fire*, **13**, 49–63, doi:10.1071/WF03043.
- Clements, C. B., B. E. Potter, and S. Zhong, 2006: In situ Measurements of Water Vapor, Heat and CO₂ Fluxes within a prescribed Grass Fire. *International Journal of Wildland Fire*, **15**(3), 299–306, doi:10.1071/WF05101.
- Coen, J. L., T. L. Clark, and D. Latham, 2001: Coupled atmosphere-fire model simulations in various fuel types in complex terrain. In 4th. Symp. Fire and Forest Meteor. Amer. Meteor. Soc., Reno, Nov. 13–15, pages 39–42.
- Countryman, C. M., 1969: PROJECT FLAMBEAU - An Investigation of Mass Fires (1964–1967), Final Report - Volume I. Pacific Southwest Forest and Range Experiment Station, Berkeley, CA.
- Cuxart, J., P. H. Bougeault, and J. L. Redelsperger, 2000: A turbulence scheme allowing for mesoscale and large-eddy simulations. *Q. J. R. Meteorol. Soc.*, **126**, 1–30, doi:10.1002/qj.49712656202.
- Du, J., B. Fix, J. Glimm, X. Jia, X. Li, Y. Li, and L. Wu, 2006: A simple package for front tracking. *Journal of Computational Physics*, **213**(2), 613–628, doi:10.1016/j.jcp.2005.08.034.
- Heilman, W. E., and J. D. Fast, 1992: Simulations of Horizontal Roll Vortex Development Above Lines of Extreme Surface Heating. *International Journal of Wildland Fire*, **2**, 55–68, doi:10.1071/WF9920055.
- Knight, I. K., and A. L. Sullivan, 2004: A semi-transparent model of bushfire flames to predict radiant heat flux.

- International Journal of Wildland Fire*, **13**, 201–207, doi:[10.1071/WF03047](https://doi.org/10.1071/WF03047).
- Lafore, J. P., J. Stein, N. Asencio, P. Bougeault, V. Ducrocq, J. Duron, C. Fischer, P. Hereil, P. Mascart, J. P. Pinty, J. L. Redelsperger, E. Richard, and J. Vila-Guerau de Arellano, 1998: The Meso-NH Atmospheric Simulation System. Part I: Adiabatic formulation and control simulations. *Annales Geophysicae*, **16**, 90–109, doi:[10.1007/s00585-997-0090-6](https://doi.org/10.1007/s00585-997-0090-6).
- Lallemand, P., L. Luo, and Y. Pengb, 2007: A lattice Boltzmann front-tracking method for interface dynamics with surface tension in two dimensions. *Journal of Computational Physics*, **226**(2), 1367–1384, doi:[10.1016/j.jcp.2007.05.021](https://doi.org/10.1016/j.jcp.2007.05.021).
- Linn, R.R., J. Reisner, J. Colman, and J. Winterkamp, 2002: Studying Wildfire Using FIRETEC. *International Journal of Wildland Fires*, **11**, 1–14, doi:[10.1071/WF02007](https://doi.org/10.1071/WF02007).
- Linn, R. R., J. Winterkamp, C. Edminster, J. J. Colman, and W. S. Smith, 2007: Coupled influences of topography and wind on wildland fire behaviour. *International Journal of Wildland Fire*, **16**, 183–195, doi:[10.1071/WF06078](https://doi.org/10.1071/WF06078).
- McCaffrey, B.J., 1986: Momentum Implications for Buoyant Diffusion Flames. *Comb. and Flame*, **52**, 149–67, doi:[10.1016/0010-2180\(83\)90129-3](https://doi.org/10.1016/0010-2180(83)90129-3).
- Masson, V., 2000: A physically based scheme for the urban energy budget in atmospheric models. *Bound. Layer Meteor.*, **94**, 357–397, doi:[10.1023/A:1002463829265](https://doi.org/10.1023/A:1002463829265).
- Mell, W., M. A. Jenkins, J. Gould, and P. Cheney, 2007: A physically based approach to modelling grassland fires. *International J. of Wildland Fire*, **16**, 1–22, doi:[10.1071/WF06002](https://doi.org/10.1071/WF06002).
- Noilhan, J., and S. Planton, 1989: A simple parameterization of land surface processes for meteorological models. *Mon. Weather Rev.*, **117**, 536–549, doi:[10.1175/1520-0493\(1989\)117<0536:ASPOLS>2.0.CO;2](https://doi.org/10.1175/1520-0493(1989)117<0536:ASPOLS>2.0.CO;2).
- Palmer, T. Y., 1969: PROJECT FLAMBEAU - An Investigation of Mass Fires (1964–1967), Final Report - Volume II: Catalogue of Project Flambeau Fires, 1964–1967. P.S.W. Forest and Range Experiment Station, Berkeley, CA.
- Quintiere, J. G., 1993: Canadian Mass Fire Experiment, 1989. *J. of Fire Prot. Engr.*, **5**(2), 67–78, doi:[10.1177/104239159300500203](https://doi.org/10.1177/104239159300500203).
- Santoni, P. A., A. Simeoni, J. L. Rossi, F. Bosseur, F. Morandini, X. Silvani, J. H. Balbi, D. Cancellieri, and L. Rossi, 2006: Instrumentation of wildland fire: characterisation of a fire spreading through a Mediterranean shrub. *Fire Safety Journal*, **41**(3), 171–184, doi:[10.1016/j.firesaf.2005.11.010](https://doi.org/10.1016/j.firesaf.2005.11.010).
- Sharples, J., 2008: Review of formal methodologies for wind–slope correction of wildfire rate of spread. *International Journal of Wildland Fire*, **17**, 179–193, doi:[10.1071/WF06156](https://doi.org/10.1071/WF06156).
- Skamarock, W. C., J. B. Klemp, 2007: A Time-Split Nonhydrostatic Atmospheric Model for Research and NWP Applications. *J. Comp. Phys.*, **227**(7), special issue on environmental modeling, doi:[10.1016/j.jcp.2007.01.037](https://doi.org/10.1016/j.jcp.2007.01.037).
- Sullivan, A. L., P. F. Ellis, and I. K. Knight, 2003: A review of the use of radiant heat flux models in bushfire applications. *International Journal of Wildland Fire*, **12**, 101–110, doi:[10.1071/WF02052](https://doi.org/10.1071/WF02052).
- Trelles, J. J., and P. J. Pagni, 1997: Fire-Induced Winds in the 20 October 1991 Oakland Hills Fire. International Association for Fire Safety Science. Fire Safety Science. Proceedings. Fifth (5th) International Symposium. March 3–7, 1997, Melbourne, Australia, Intl. Assoc. for Fire Safety Science, Boston, MA, Hasemi, Y., Editor(s), 911–922 pp.
- Rothermel, R. 1972: A mathematical model for predicting fire spread in wildland fuels. Research Paper INT-115, USDA Forest Service.
- Woodward, P. R., and P. Colella, 1984: The piecewise Parabolic Method (PPM) for gas dynamical simulations. *J. Comput. Phys.*, **54**, 174–201, doi:[10.1016/0021-9991\(84\)90143-8](https://doi.org/10.1016/0021-9991(84)90143-8).